

# Collective excitations and confinement in the excitation spectra of the spinless fermion model on a ladder

K. Yonemitsu

*Institute for Molecular Science and Graduate University for Advanced Studies, Okazaki 444-8585, Japan*

(Received 16 August 2001; revised manuscript received 18 March 2002; published 31 July 2002)

Intrachain and interchain local charge-transfer excitation spectra and the single-particle density of states are calculated in the spinless fermion model on a ladder with varying intrachain nearest-neighbor repulsion and interchain transfer integral at and near half filling by using the finite-temperature density-matrix renormalization-group method. Collective excitations are found to govern the low-energy intrachain spectra, while only individual local excitations are present in the interchain spectra. For strong intrachain repulsion, the low-energy motion of fermions is confined within a chain. The interchain motion of fermions is not bandlike but incoherent. As a consequence, the low-energy intrachain spectra are sensitive at half filling to the interchain transfer integral that weakens the density-density correlation along the chains. Similarly, the low-energy intrachain spectra are sensitive near half filling to the chemical potential that reduces the effect of the umklapp process. Similarities are pointed out between these findings and the experimentally observed, optical conductivity spectra in the quasi-one-dimensional organic conductors (TMTSF)<sub>2</sub>X.

DOI: 10.1103/PhysRevB.66.035121

PACS number(s): 78.40.Me, 74.70.Kn, 71.30.+h, 72.15.Nj

## I. INTRODUCTION

Electron correlation brings about exotic electronic phases in quasi-one-dimensional organic conductors (TMTTF)<sub>2</sub>X (TMTTF=tetramethyltetrafulvalene), (TMTSF)<sub>2</sub>X (TMTSF=tetramethyltetraselenafulvalene), and many others.<sup>1,2</sup> In addition to the presence of a variety of broken-symmetry ground states, dimensional crossovers observed in normal states above the transition temperatures have attracted much attention.<sup>3</sup> In general, dimensional crossovers are achieved either through one-particle processes or through two-particle ones.<sup>4-6</sup> Without commensurability or an internal structure, a one-dimensional Tomonaga-Luttinger liquid is easily destabilized by interchain one-particle hopping processes and replaced by a Fermi liquid.<sup>7</sup> However, the umklapp process<sup>8</sup> or a two-leg-ladder structure<sup>9</sup> suppresses the interchain or interladder one-particle processes to cause a transition through two-particle processes often from a non-Fermi-liquid state (such as a charge-localized state<sup>10</sup> or a spin-gap metal,<sup>11</sup> respectively) to a long-range-ordered state (such as an antiferromagnet<sup>12,13</sup> or superconductor,<sup>14</sup> respectively). Studies of the crossover from the Tomonaga-Luttinger liquid to the Fermi liquid and related subjects are actively ongoing.<sup>15-19</sup>

The frequency dependence of the optical conductivity in (TMTTF)<sub>2</sub>X and (TMTSF)<sub>2</sub>X has been extensively studied for the electric field polarized along each direction.<sup>10</sup> For polarization perpendicular to the chains, a plasma edge is absent in (TMTTF)<sub>2</sub>X, while it is present in (TMTSF)<sub>2</sub>X, suggesting that electrons are confined into the chains in the former and delocalized over the chains in the latter. Thus the interchain excitation spectra are modified by small changes in the interchain transfer integral  $t_b$  and/or the degree of dimerization, i.e., the strength of the intrachain umklapp process.

Dimensional crossovers are observed also in the excitation spectra with fixed pressure and temperature when

viewed as a function of energy.<sup>20</sup> (TMTSF)<sub>2</sub>CIO<sub>4</sub> at a low temperature  $T \sim 10$  K is located on the “high-pressure” (thus high-dimensional) side of the phase diagram. Around  $\omega \sim 100$  meV, the optical excitations are confined in the  $a$  axis and show a power-law behavior characteristic of a Tomonaga-Luttinger liquid. But there are pseudogap structures around  $\omega \sim 30$  meV (6 meV) in the  $a$ - ( $b$ -) axis spectra. At very low energies,  $\omega \lesssim 0.1$  meV, the optical conductivity becomes rather isotropic, Drude-like, showing the character of a two- or three-dimensional metal. Thus, the effective dimensionality may be regarded as raised at very low energies in the metallic phase.

In the simplest renormalization-group theories for one-dimensional systems, the logarithmic singularity is cut off by either finite temperature or finite energy.<sup>21</sup> Then, varying energy scales are often treated by varying temperatures, or vice versa. However, even in much more tractable, quantum Ising and rotor models, for instance, the critical properties around the quantum phase transition have shown complex behavior depending on temperature and on energy.<sup>22</sup> Here we approach crossovers in excitation spectra of quasi-one-dimensional systems by a method called the transfer-matrix renormalization-group (TMRG) or finite-temperature density-matrix renormalization-group (finite- $T$  DMRG) method.<sup>23-25</sup> This method has been extended from the (ground-state) DMRG method for Hamiltonians<sup>26</sup> and applied to quantum transfer matrices for periodic one-dimensional systems with infinite length and at finite temperatures. Although the information about dynamical properties is limited to spatially local (thus containing all the wave-number components) correlations, we find different characteristics between intrachain and interchain excitations around a quantum phase transition.

As a first step toward quasi-one-dimensional electron systems, we adopt the spinless fermion model on a two-leg ladder near half filling. We show that, for strong intrachain repulsion, the low-energy motion of fermions is confined

within a chain. The low-energy intrachain spectra are then sensitive to the interchain transfer integral and to the chemical potential. We interpret these findings with collective motion of solitons and antisolitons along the chains, and with individual motion of fermions across the chains.

## II. SPINLESS FERMIONS ON A LADDER

The spinless fermion model we use is written as

$$H = -t \sum_i \sum_{j=1}^2 (c_{i,j}^\dagger c_{i+1,j} + \text{H.c.}) - t_b \sum_i (c_{i,1}^\dagger c_{i,2} + \text{H.c.}) + V \sum_i \sum_{j=1}^2 \delta n_{i,j} \delta n_{i+1,j} - \mu \sum_i \sum_{j=1}^2 n_{i,j}, \quad (1)$$

where  $c_{i,j}^\dagger$  ( $c_{i,j}$ ) creates (annihilates) a spinless fermion on the  $i$ th site of the  $j$ th leg,  $n_{i,j} = c_{i,j}^\dagger c_{i,j}$ , and  $\delta n_{i,j} = n_{i,j} - 1/2$ . The intrachain and interchain transfer integrals are denoted by  $t$  and  $t_b$ , respectively, the intrachain nearest-neighbor repulsion strength by  $V$ , and the chemical potential by  $\mu$ . We consider half filling,  $\mu = 0$ , unless we explicitly state otherwise. The doping effect is studied at last.

The excitation spectra with respect to one- and two-body correlation functions are obtained by analytic continuation of the corresponding imaginary-time-dependent correlation functions. For a one-body correlation function, we calculated the single-particle density of states  $\rho(\omega) = -(1/\pi) \text{Im}G(\omega + i\delta)$ , where  $G(\tau) = -\langle c_{i,j}(\tau) c_{i,j}^\dagger(0) \rangle$  for  $0 < \tau < \beta$  with the inverse temperature  $\beta$ . For two-body correlation functions, we calculated the corresponding dynamical structure factors, following Ref. 25,  $S_{AB}(\omega) = -(1/\pi) \text{Im}\chi_{AB}(\omega + i\delta)/(1 - e^{-\beta\omega})$ , where  $\chi_{AB}(\tau) = -\langle A(\tau) B^\dagger(0) \rangle$  for  $0 < \tau < \beta$ . We adopt  $A = B = j_{x,i,j} \equiv i(c_{i,j}^\dagger c_{i+1,j} - c_{i+1,j}^\dagger c_{i,j})$  and  $A = B = j_{y,i} \equiv i(c_{i,1}^\dagger c_{i,2} - c_{i,2}^\dagger c_{i,1})$  for the local charge-transfer processes along and across the chains, respectively. For the Trotter number with which the quantum transfer matrix is decomposed, we take  $M = 30$ . For the number of states kept in the DMRG technique, we take  $m = 26, 28, \text{ or } 30$ . The temperature  $T$  we used is  $0.25t$ . Numerical errors from these finite  $m$  values are found to be larger than those from the Trotter decomposition. From comparisons between data for these and smaller  $m$  values, however, we find that the conclusions are not altered by the numerical errors.

The single-chain model, which corresponds to  $t_b = 0$  in the two-leg ladder model, is treated at half filling in Appendix A. It is equivalent to the spin-1/2 XXZ model, so that its ground-state property is exactly known from the Bethe ansatz: it is metallic and uniform for  $V < V_c = 2t$ , while it is insulating for  $V > V_c$  because of density alternation. The single-particle densities of states and the dynamical structure factors for the local charge transfer (along the chain) shown there can be used as the data for  $t_b = 0$ . We have also checked the influence of taking different  $m$  and  $M$  values in Appendix A, which shows good convergence. In the present two-leg ladder model, the convergence becomes worse so that one should expect that the presented data show qualitative overall tendencies. The dynamical structure factors in

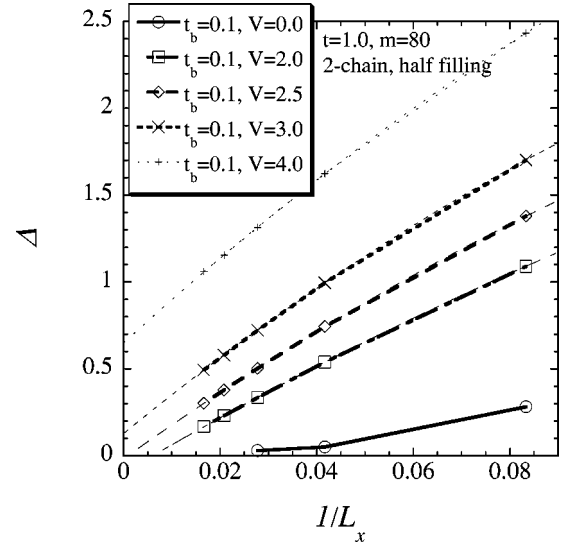


FIG. 1. Gap calculated by the ground-state DMRG for finite systems with chain length  $L_x$ , for different  $V$  and  $t_b = 0.1$  at half filling. The other parameters are  $t = 1.0$  and  $m = 80$ .

the two-leg ladder model are also shown for different  $m$  values in Appendix A for comparison. Below we will state so if we encounter such artifacts that have not been obtained systematically with different  $m$  and  $M$  values.

## III. RESULTS

### A. Static properties

Before calculating the excitation spectra, we first use the ordinary ground-state DMRG method to see the static and spatial properties of finite-sized two-leg-ladder systems with chain length  $L_x$  (in the unit of lattice spacing) and the open boundary condition. The magnitude of the gap, defined by  $\Delta \equiv E(L_x - 1) + E(L_x + 1) - 2E(L_x)$  with  $E(n)$  being the ground-state energy for  $n$  fermions, is shown in Figs. 1 and 2 as a function of  $1/L_x$ . For  $t_b = 0$ , the quantum phase transition takes place at  $V_c = 2t$ : the ground state is metallic for  $V < V_c$  and insulating for  $V > V_c$ . The gap decreases with increasing  $t_b$  for each  $L_x$  as shown in Fig. 2, so that  $V_c$  would increase with  $t_b$  in the  $L_x \rightarrow \infty$  limit. For  $t_b = 0.1$ ,  $V_c$  is about 2.5 as shown in Fig. 1. The data for  $t_b = 0.1$  here with  $m = 120$  are hardly distinguishable from those with  $m = 60, 80, \text{ and } 100$ .<sup>27</sup> With increasing  $t_b$ , the truncation error becomes large because the wave function is numerically represented on site bases. Then, the data for large  $t_b$  and small  $1/L_x$  may suffer from the problem of getting stuck in metastable states.<sup>28</sup> We can say, at least, the gap for  $V = 3.0$  becomes substantially small for  $t_b \geq 0.3$ , while the gap for  $V = 4.0$  survives for  $t_b \leq 0.4$  [note the different origins of the vertical axes in Figs. 2(a) and 2(b)]. Looking at the density-density correlation functions (not shown), we find that the insulator phase has a checkerboard pattern of charge order as shown in Fig. 3. As described later, the charge order in the insulating phase is reflected by individual modes appearing in dynamical structure factors.

It was recently claimed, using bosonization with the perturbative renormalization-group method, that the two-leg

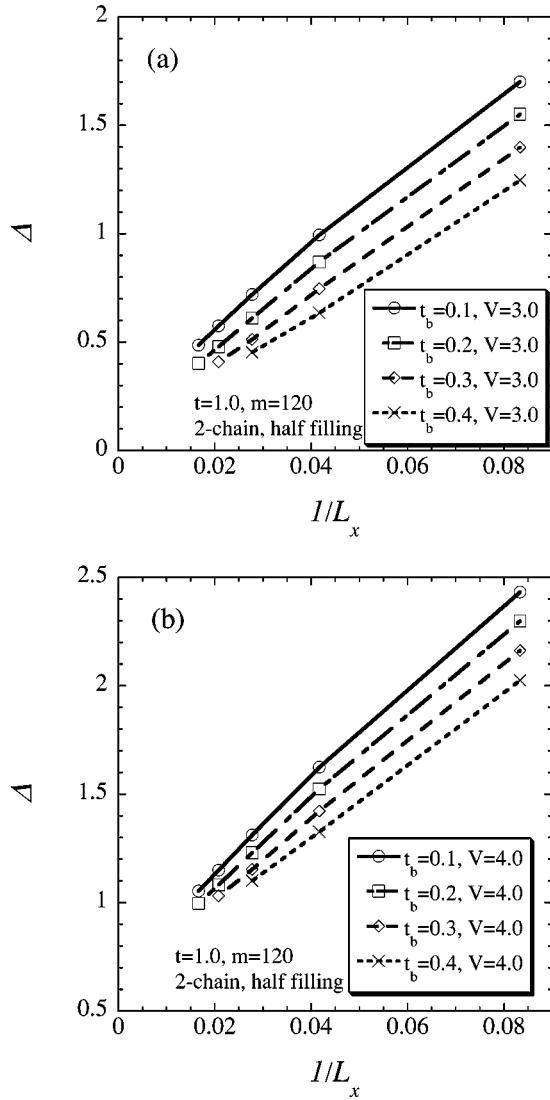


FIG. 2. Gap calculated by the ground-state DMRG for finite systems with chain length  $L_x$ , for different  $t_b$ , (a) for  $V=3.0$ , and (b) for  $V=4.0$ , at half filling. The other parameters are  $t=1.0$  and  $m=120$ .

ladder of spinless fermions at half filling becomes a Mott insulator for arbitrary weak repulsive interactions.<sup>29</sup> Thus, it is inconsistent with the results described above. Since both this analytic work and the present numerical approach have their own drawbacks, we here discuss the origin of the dif-

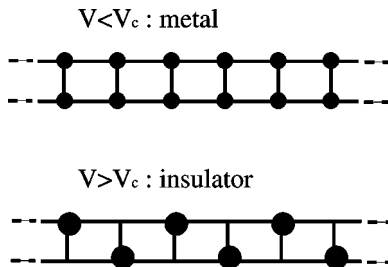


FIG. 3. Schematic ground states in the metallic phase for  $V < V_c$ , and in the insulating phase for  $V > V_c$ .

ference. For  $V < 2t$ , the system is gapless and uniform at  $t_b = 0$ . The addition of the  $t_b$  term would reduce the total energy by kinetic energy gain. Then, it seems reasonable to expect that the fermions tend to be more delocalized and that the charge order remains destabilized. At least for finite systems up to  $L_x=60$ , the gap due to the finite-size effect always becomes smaller with increasing  $t_b$ . It seems to hold when the data are extrapolated to  $L_x=\infty$ . It is noted that this argument based on the kinetic energy gain does not always applicable: for the infinite number of chains and with spin 1/2, the long-range antiferromagnetic order is stabilized (i.e., the continuous symmetry is broken) only when  $t_b \neq 0$ , so that the fermions are not always delocalized by  $t_b$ . In the present case of spinless fermions, however, the charge order is present (i.e., the discrete symmetry is broken) for  $V > 2t$  in the ground state even when  $t_b=0$ , so that the situation is different from the spin-1/2 case.

In the bosonization argument, the scaling dimension of the umklapp term is essential. For  $t_b=0$ , it is  $2-4K$  with the Tomonaga-Luttinger parameter  $K$  ( $K < 1$  for repulsive interactions). The charge gap is produced for  $K < 1/2$ , i.e., for sufficiently strong repulsive interactions. The interchain  $t_b$  term proportional to  $-t_b \cos(\sqrt{2}\phi_a)\cos(\sqrt{2}\theta_a)$ , where  $\phi_a = (\phi_1 - \phi_2)/\sqrt{2}$ ,  $\theta_a = (\theta_1 - \theta_2)/\sqrt{2}$ ,  $\phi_j$  and  $\theta_j/\pi$  are conjugate phase operators for chain  $j=1,2$ , is coupled with the umklapp term proportional to  $-g_u \cos(\sqrt{8}\phi_a)\cos(\sqrt{8}\phi_s)$ , where  $\phi_s = (\phi_1 + \phi_2)/\sqrt{2}$ . Then a new term proportional to  $\cos(\sqrt{8}\phi_s)$  is generated during the renormalization procedure, which has the scaling dimension  $2-2K_s$  and becomes relevant for  $K_s < 1$ .<sup>29</sup> This argument seems reasonable, but the argument for the interchain  $t_b$  term must always be accompanied. The latter term has the scaling dimension  $2-(K_a + 1/K_a)/2$ , which is much larger than that of the umklapp term for weak repulsive interactions. In other words, the scaling law may break down. In such a case, the tendency toward delocalization usually dominates, so that another regime controls the low-energy properties.<sup>19</sup>

Once the scaling argument is assumed to hold, then the charge gap becomes finite but very small.<sup>29</sup> For small  $t_b$ , it becomes the infinitely large power of  $t_b$  (thus it vanishes faster than the standard Berezinskii-Kosterlitz-Thouless behavior). For small  $V$  and large  $t_b$ , it again becomes the infinitely large power of  $V$ ,  $\sim V^{\text{const}/V}$ . It is then logically possible that the present numerical approach misses to pick up such a tiny gap. Numerically, we encounter unstable behavior when we further increase the Trotter number  $M$ , so that we cannot pick it up. The energy scale  $\omega$  discussed later is not so small, so that the later discussions are not affected at all even if the tiny gap is present. Then, the results shown below would correspond to the confinement-deconfinement crossover inside the insulator phase of Ref. 29. Our previous finite- $T$  DMRG study suggests that, for small  $V$ , the density deviates from the half as soon as the chemical potential becomes finite.<sup>30</sup> It would be very hard in any case to numerically observe the gap for small  $V$  since its magnitude is very small, if present.

## B. Intrachain correlation effects

Hereafter, we show numerical results obtained by the finite- $T$  DMRG method combined with the analytic continu-

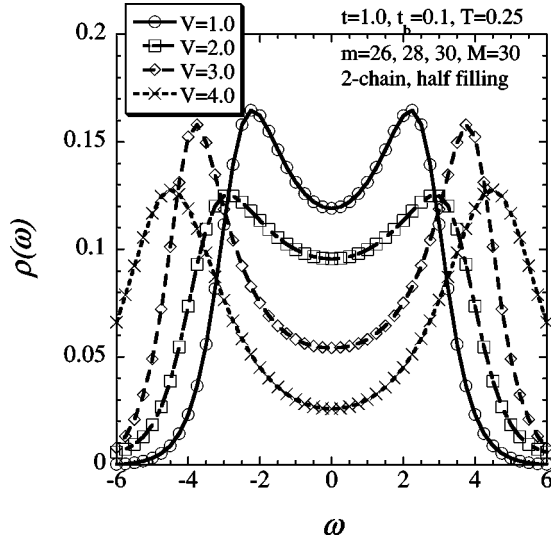


FIG. 4. Density of states for different  $V$  and  $t_b=0.1$  at half filling. The other parameters are  $t=1.0$ ,  $T=0.25$ ,  $m=26, 28$ , or  $30$ , and  $M=30$ . The larger  $m$  is used for the more singular spectrum at the smaller  $V$ .

ation from the imaginary-frequency axis to the real-frequency axis. Figure 4 shows the single-particle density of states  $\rho(\omega)$  for different  $V$ . For  $V=0$  and at zero temperature (not shown),  $\rho(\omega)$  is known to have the inverse-square-root singularities near  $\omega = \pm 2t$ . For small  $V$  and at low temperatures, the singularities are rounded, but their remnant clearly appears near  $\omega = \pm 2t$ . With increasing  $V$ ,  $\rho(\omega)$  at the chemical potential ( $\omega=0$  at half filling) quickly decreases. For  $V=4.0$ , there is an energy gap of about 0.6 according to Figs. 1 and 2(b), but it is not clearly seen even at  $T=0.25$  presumably because  $m$  is not large enough. With increasing  $V$ , the peak at  $\omega > 0$  is shifted to higher energies, and that at  $\omega < 0$  to low energies at half filling.<sup>31</sup> For large  $V$ , the peaks are located roughly at  $\omega = \pm V$ . This is understood from the

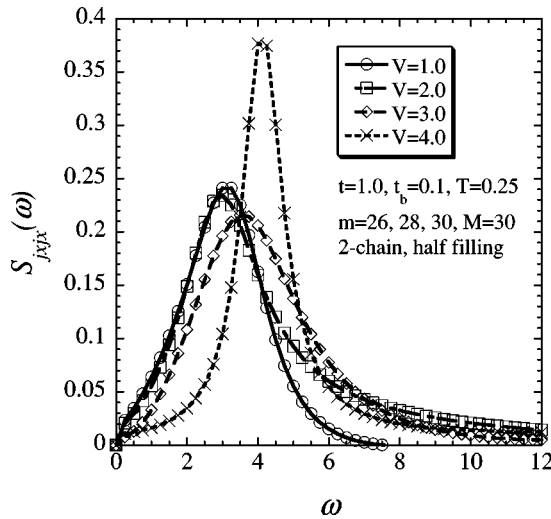


FIG. 5. Dynamical structure factor for the local charge transfer along the chains, for different  $V$  and  $t_b=0.1$  at half filling. The other parameters are  $t=1.0$ ,  $T=0.25$ ,  $m=26, 28$ , or  $30$ , and  $M=30$ .

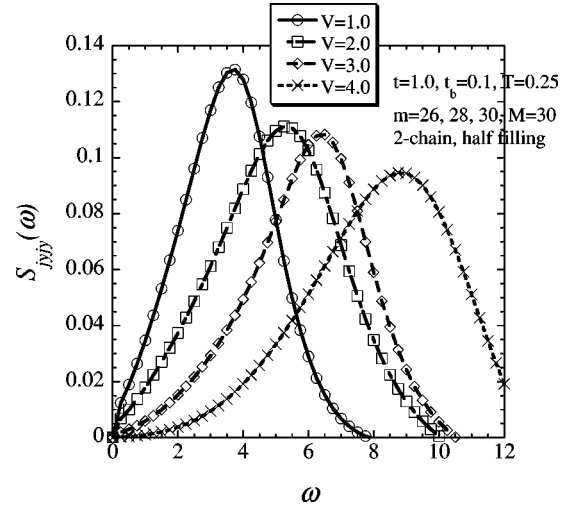


FIG. 6. Dynamical structure factor for the local charge transfer across the chains, for different  $V$  and  $t_b=0.1$  at half filling. The other parameters are  $t=1.0$ ,  $T=0.25$ ,  $m=26, 28$ , or  $30$ , and  $M=30$ .

particle-hole symmetry and the fact that the energy of  $2V$  is required in the strong-coupling limit  $V \rightarrow \infty$ , to add a fermion to the half-filled system.

The dynamical structure factors for the local charge transfer *along the chains*  $S_{jyx}(\omega)$  are shown in Fig. 5. Their behavior is in sharp contrast to that of the dynamical structure factors for the local charge transfer *across the chains*  $S_{jyy}(\omega)$  shown in Fig. 6 below. Recall that, for  $t_b=0.1$ , the system is metallic and gapless for  $V < V_c \approx 2.5$ , while it is an insulator with a finite gap for  $V > V_c$ . The intrachain spectra  $S_{jyx}(\omega)$  are insensitive to  $V$  for  $V < V_c$ . It is similar to the single-chain case shown in Appendix A. The low-energy side of the peak is almost independent of  $V$ , though the high-energy side is gradually extended to further higher energies with increasing  $V$ . Meanwhile, in the insulating phase for  $V > V_c$ , the magnitude of the gap at  $t_b=0.1$  is about 0.1 for  $V=3.0$  and about 0.6 for  $V=4.0$ .<sup>27</sup> The growth of the gap with increasing  $V$  for  $V > V_c$  is reflected in the low-energy part of the spectra. The spectral weight is suppressed further beyond the gap. It may be regarded as a pseudogap. For large  $V$ , the pronounced peak appears at around  $\omega = V$ . This is due to the intrachain charge-transfer modes shown in Fig. 7. In the strong-coupling limit, the charge-order pattern is as shown in Fig. 3 for  $V > V_c$ . Then the energies of these modes

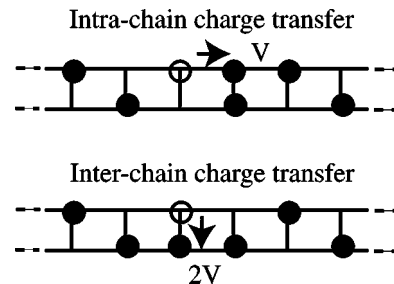


FIG. 7. Intrachain and interchain local charge-transfer processes, which approximately cost  $V$  and  $2V$ , respectively.

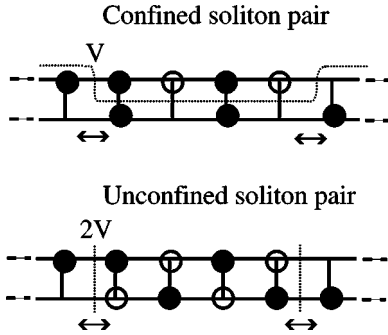


FIG. 8. Confined and unconfined pairs of solitons, which move collectively.

are given by  $V$  because the number of nearest-neighbor pairs along the chains is increased by 1. These modes are individual and locally excited.

The interchain spectra  $S_{jyjy}(\omega)$  show different behavior (Fig. 6). The low-energy part of  $S_{jyjy}(\omega)$  steadily loses the spectral weight with increasing  $V$ , and shows a large pseudogap structure for  $V > V_c$ . Compared with  $S_{jxjx}(\omega)$ ,  $S_{jyjy}(\omega)$  are much more sensitive to  $V$  in the whole energy range. For large  $V$ , the pronounced peak now appears at around  $\omega = 2V$ . This is due to the interchain charge-transfer modes shown in Fig. 7. This time the corresponding energies are given by  $2V$  in the strong coupling limit because the number of nearest-neighbor pairs along the chains is increased by 2. These modes are also individual and locally excited. Compared with  $S_{jxjx}(\omega)$ , the spectral weight is shifted to higher energies as a whole and the pseudogap structure is more extended.

To clarify the origin of the significant difference between  $S_{jxjx}(\omega)$  and  $S_{jyjy}(\omega)$ , we consider collective modes that become important at low energies. There are two types of soliton pairs for  $V > V_c$ , as shown in Fig. 8. Note that the checkerboard pattern is stabilized by the superexchange processes of fermions along the rungs. When the charge-order configuration of any finite length within a chain is shifted by one lattice constant, a pair of a soliton and an antisoliton is created. It costs about  $V$  at most because the number of nearest-neighbor pairs along the chains is increased by only 1. The quantum fluctuations of the positions of the solitons reduce the energy cost. Because of the mismatch between the neighboring chains, some superexchange processes are disallowed, so that the energy of the soliton pair increases linearly with the distance between the soliton and the antisoliton. The soliton and the antisoliton are not freely propagating but confined at half filling. It is noted that ‘‘confinement’’ here describes the motion of the solitons that is not free from the antisolitons. In this paper, ‘‘confinement’’ is mainly used for the motion of the fermions that is forced along the chains. When the charge-order configuration is shifted simultaneously on both of the chains by one lattice constant, the soliton pair does not suffer from the confinement, but their energy cost reaches about  $2V$ . The kinetic energy gain from the fluctuating locations of the solitons is much smaller than that for the confined soliton pair. They would be less important than the confined soliton pairs. In short, the low-energy

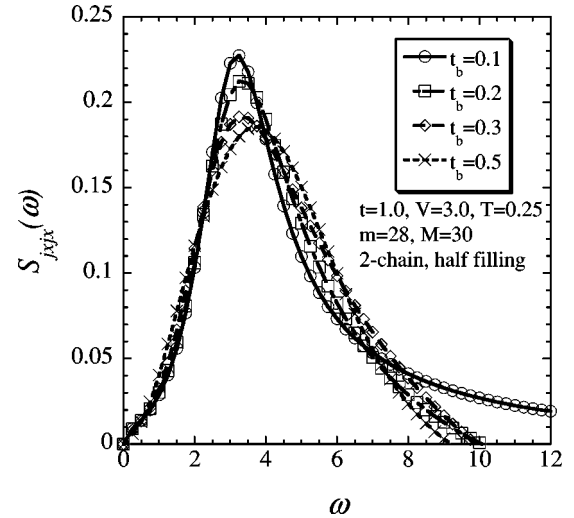


FIG. 9. Dynamical structure factor for the local charge transfer along the chains, for different  $t_b$  and  $V=3.0$  at half filling. The other parameters are  $t=1.0$ ,  $T=0.25$ ,  $m=28$ , and  $M=30$ .

charge-transfer excitations would be governed by solitons. With decreasing  $V$ , the creation energies of soliton pairs are reduced.

For  $V < V_c$ , the charge order does not exist statically as a truly long-ranged order. However, even in this uniform phase, there exists a short-range charge-order correlation, which grows with  $V$ . Therefore, with increasing  $V$ , the motion of solitons has a more collective character, and becomes important at low energies. Note that the solitons can propagate along the chains: they can be excited only within a chain so that they are reflected only in  $S_{jxjx}(\omega)$ . This makes the significant difference between  $S_{jxjx}(\omega)$  and  $S_{jyjy}(\omega)$ . In other words, the low-energy part of  $S_{jxjx}(\omega)$  does not change so much, but the modes contributing to the low-energy part gradually change their characters from individual to collective ones. Meanwhile, the collective modes are missing in  $S_{jyjy}(\omega)$ , so that they cannot fill the low-energy part. The charge-transfer processes take place incoherently across the chains. A fermion transferred across the chains would then feel so large change in the local environment that the corresponding interchain spectrum is thus sensitive to  $V$ . In other words, the intrachain interaction  $V$ , which controls mainly the intrachain correlation, modifies the interchain local charge-transfer excitation spectra much more sensitively than the intrachain spectra.

### C. Interchain overlap effects

Now we study how the intrachain spectrum  $S_{jxjx}(\omega)$  evolves with  $t_b$ . For  $V$  below the critical strength  $V_c$ , the low-energy part of  $S_{jxjx}(\omega)$  is found to be insensitive to  $t_b$  (not shown). The high-energy part is only slightly extended to further higher energies because the band becomes broad with increasing  $t_b$ . For  $V$  just above the critical strength  $V_c$ , the  $t_b$  dependence of the intrachain spectrum  $S_{jxjx}(\omega)$  is shown in Fig. 9. It is noted that the magnitude of the gap is about 0.1 at most and smaller than the temperature  $T=0.25$ . In contrast to the small- $V$  case, however, the low-energy

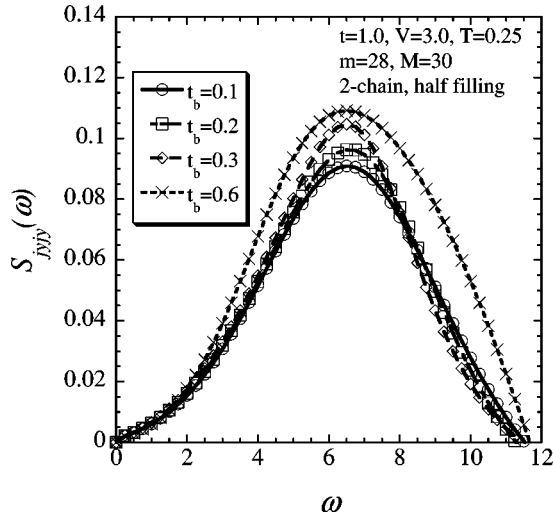


FIG. 10. Dynamical structure factor for the local charge transfer across the chains, for different  $t_b$  and  $V=3.0$  at half filling. The other parameters are  $t=1.0$ ,  $T=0.25$ ,  $m=28$ , and  $M=30$ .

spectrum (at  $\omega \lesssim 2$ ) slightly but steadily grows with  $t_b$ . For  $V$  much above the critical strength  $V_c$ , the pseudogap in  $S_{jxjx}(\omega)$  at low energies is filled, and consequently the spectral weight increases with  $t_b$  (not shown). This indicates that the atomic picture shown in Fig. 7 for the individual modes does not hold for large  $t_b$ . The increasing  $t_b$  reduces the charge-order correlation and facilitates the collective charge-transfer excitations. Such evolution with  $t_b$  at low energies is not found in  $S_{jyjy}(\omega)$ . That is, the interchain transfer integral  $t_b$  modifies the intrachain local charge-transfer excitation spectra much more sensitively than the interchain spectra at low energies.

Evolution of the interchain spectrum  $S_{jyjy}(\omega)$  with  $t_b$  is then studied. For  $V$  below the critical strength  $V_c$ , the low-energy part of  $S_{jyjy}(\omega)$  is insensitive to  $t_b$  (not shown). For  $V$  just above the critical strength  $V_c$ , the interchain spectra  $S_{jyjy}(\omega)$  are shown in Fig. 10. The low-energy spectral weight remains suppressed when  $t_b$  increases. This behavior is reminiscent of confinement in the context of coupled Tomonaga-Luttinger liquids. It has been argued on the basis of the perturbative renormalization-group theory that the Mott gap prohibits coherent interchain one-particle hopping in  $(\text{TMTTF})_2\text{X}$ .<sup>32</sup> A confinement-deconfinement transition with increasing  $t_b$  is also studied by applying the bosonization technique to the half-filled, two coupled chains with a misfit parameter due to the interchain one-particle hopping.<sup>33</sup> Ground-state DMRG studies for three coupled extended Hubbard chains show results consistent with this view.<sup>34</sup> At low energies, fermions are confined in the chains, so that they cannot be freely transferred by the interchain local charge-transfer operator. Thus, the low-energy part of  $S_{jyjy}(\omega)$  is almost independent of  $t_b$ . Since the fermions are more strongly confined for smaller  $t_b$ , the difference between  $S_{jyjy}(\omega)$  and the single-chain spectrum appears at higher energies. With increasing  $t_b$ , the confinement becomes weak, so that  $S_{jyjy}(\omega)$  starts to deviate from the single-chain spectrum from the lower energy (thus in the wider energy range). For  $V$  much above the critical strength

$V_c$ , the confinement behavior of the interchain spectra  $S_{jyjy}(\omega)$  is again observed (not shown). Now  $V$  is larger, so that the pseudogap structure ranges wider, and the confinement is stronger. Then, a wider range of the low-energy part in  $S_{jyjy}(\omega)$  is almost independent of  $t_b$ , compared with  $S_{jxjx}(\omega)$  just above the critical strength  $V_c$ . The spectra  $S_{jyjy}(\omega)$  are enhanced by  $t_b$  only at high energies,  $\omega \gtrsim 4$ , which is much larger than the magnitude of the gap of about 0.6 at most.

#### D. Doping effects

Hereafter we consider the effect of doping by shifting the chemical potential from zero. At  $t=1.0$ ,  $t_b=0.1$ ,  $T=0.25$ , and for  $\mu=0.0, 0.4, 1.0, 1.5$ , the density per site respectively becomes 0.500, 0.538, 0.599, 0.660 for  $V=1.0$  ( $<V_c$ ); 0.500, 0.514, 0.538, 0.563 for  $V=3.0$  ( $\geq V_c$ ); and 0.500, 0.505, 0.518, 0.535 for  $V=4.0$  ( $>V_c$ ). Here  $V_c$  denotes the critical strength at half filling. With increasing  $V$ , the density increases more slowly with  $\mu$ . Below we show how the dynamical structure factors change with  $\mu$ . Roughly speaking, their dependence on  $\mu$  is similar to that on  $t_b$  especially for  $V > V_c$ . Later we will discuss why the similarity appears. At half filling, solitons are present basically in the excited states only. Meanwhile, away from half filling, solitons are always present in the ground states. Their translational motion can be viewed as Goldstone modes, which make the system metallic. The charge gap for large  $V$  at half filling persists when  $t_b$  increases, but it disappears upon doping. Therefore, the similarity between the  $\mu \neq 0$  and  $t_b \neq 0$  cases should be understood carefully.

Evolution of the intrachain spectrum  $S_{jxjx}(\omega)$  with  $\mu$  is studied. For  $V$  below the critical strength, the low-energy part of  $S_{jxjx}(\omega)$  is found to be insensitive to  $\mu$  (not shown). As  $\mu$  deviates from zero, higher-energy excitations become possible, so that the high-energy part is slightly shifted to further higher energies. For  $V$  just above the critical strength  $V_c$ , the growth of the low-energy spectral weight with  $\mu$  is clearly seen in Fig. 11. The peak is shifted to higher energies with increasing  $\mu$ . For  $V$  much above the critical strength  $V_c$ , the filling in the low-energy pseudogap and the consequent growth of the low-energy spectral weight quickly take place with increasing  $\mu$  (not shown). Somewhat similar behavior is found in  $S_{jyjy}(\omega)$  also, but its dependence on  $\mu$  is much weaker than that in  $S_{jxjx}(\omega)$ . For  $V > V_c$ , the low-energy excitations are attributed to the motion of solitons. Away from half filling, they are always present in the ground states. With increasing  $\mu$ , the density of solitons increases, so that the charge-order correlation is weakened, facilitating the collective charge-transfer excitations. Because solitons move along the chains, the growth of the low-energy spectral weight appears mainly in  $S_{jxjx}(\omega)$ .

Evolution of the interchain spectrum  $S_{jyjy}(\omega)$  with  $\mu$  is finally studied. For  $V$  below the critical strength  $V_c$ , the low-energy part of  $S_{jyjy}(\omega)$  slowly increases with  $\mu$  (not shown). The high-energy part is shifted to further higher energies as in  $S_{jxjx}(\omega)$ . For  $V$  just above the critical strength  $V_c$ , the growth of the low-energy spectral weight with  $\mu$  is clearly seen in Fig. 12. It is not so strongly suppressed as in

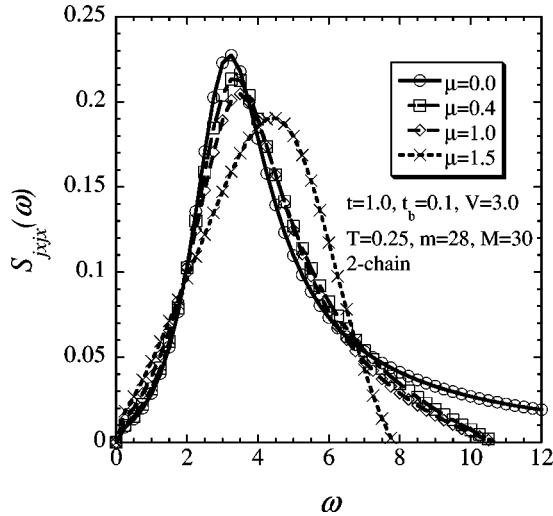


FIG. 11. Dynamical structure factor for the local charge transfer along the chains, for different  $\mu$  at and near half filling with  $V = 3.0$  and  $t_b = 0.1$ . The other parameters are  $t = 1.0$ ,  $T = 0.25$ ,  $m = 28$ , and  $M = 30$ .

the case of increasing  $t_b$  at half filling. The difference between the  $\mu \neq 0$  and  $t_b \neq 0$  cases would be due to the fact that solitons are present in the ground states in the former, while they are absent in the latter. For  $V$  much above the critical strength  $V_c$ , the slight growth of the low-energy spectral weight with  $\mu$  is seen (not shown). However, it is weaker than the case just above the critical strength  $V_c$ , and it is much weaker than that observed in  $S_{jyx}(\omega)$  for the same  $V$ . When  $V$  is large, the fermions tend to be strongly confined in the chains. Nonetheless, the low-energy spectral weight slightly increases with  $\mu$  because of the presence of solitons.

We thus find some similarities between the spectral evolution with  $t_b$  and that with  $\mu$ . For  $V > V_c$ , the evolution of the low-energy part of  $S_{jyx}(\omega)$  with  $\mu$  is faster than that

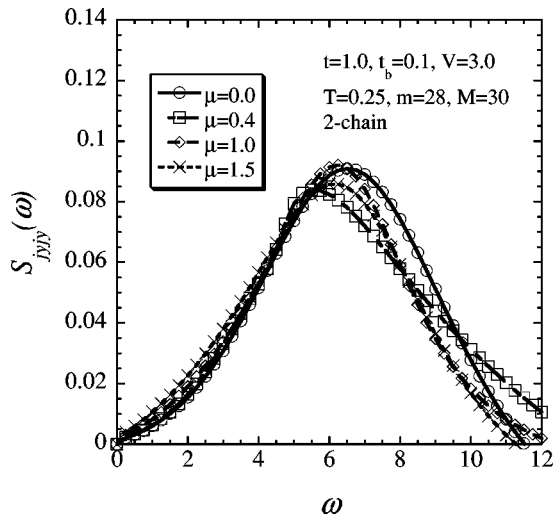


FIG. 12. Dynamical structure factor for the local charge transfer across the chains, for different  $\mu$  at and near half filling with  $V = 3.0$  and  $t_b = 0.1$ . The other parameters are  $t = 1.0$ ,  $T = 0.25$ ,  $m = 28$ , and  $M = 30$ .

with  $t_b$ , when compared with the behavior of  $S_{jyx}(\omega)$ . The similarities between the  $\mu \neq 0$  and  $t_b \neq 0$  cases may look strange at first sight. A given finite  $\mu$  is constant and does not spatially fluctuate. It changes only the averaged total number of fermions. Meanwhile, the interchain transfer integral  $t_b$  assists the interchain motion of fermions, so that the number of fermions in one chain fluctuates quantum mechanically, but the corresponding operator conserves the total number of fermions. The umklapp process due to the commensurability at half filling disfavors the quantum fluctuation of the fermion number in one chain. This is easily understood for large  $V$  from the energy cost required to transfer a fermion to the other chain at half filling. Upon doping, the commensurability is quickly lost. Then the umklapp process is so weakened that it becomes ineffective at low-energy scales. Doping does not only change the averaged total number of fermions, but also enhances the quantum fluctuation of the fermion number in one chain. That is why the doping effects are somewhat similar to the interchain overlap effects. The similarities are rather close especially for large  $V$  because the umklapp process is dominant.<sup>30</sup> In addition, the interchain transfer processes do not take place coherently owing to the gap. This situation has already been studied by the perturbative renormalization-group theory,<sup>32</sup> by the bosonization technique,<sup>33</sup> and by the ground-state DMRG method.<sup>34</sup> Once the quantum coherence in the interchain charge-transfer processes is lost, the occurrence of these processes would look as if they are statistic. Thus, this may be approximately reproduced by a thermodynamic effect of shifting the chemical potential. A similar situation is found in the optical conductivity spectra for the TMTSF family.<sup>35</sup> The observed optical features are close to those that have been calculated for a doped one-dimensional Mott insulator.<sup>36,37</sup>

#### IV. CONCLUSION AND DISCUSSION

So far, the dimensional crossover problem has been studied to clarify how the three-dimensional character of interacting fermions is achieved by increasing interchain transfer integrals: either the single-particle motion becomes coherent and the Fermi-liquid picture becomes valid, or some long-range order is developed by the interaction. Experimentally, the dimensionality is controlled not only by the physical or chemical pressure, which changes the ratios of the interchain transfer integrals to the intrachain ones, but also by the energy scale used in the measurement. In this paper, to study the correlation-driven, energy-scale-dependent “dimensional crossover,” we calculate dynamical structure factors for the local charge transfer processes along the chains and across the chains in the spinless-fermion model on a ladder at and near half filling. The finite- $T$  DMRG method is employed to treat the excitation spectra around the quantum critical point. The characters of the intrachain and interchain spectra are found very different.

Below the critical strength  $V_c$  for charge ordering, the intrachain spectra are insensitive to the intrachain repulsion, while, for any strength, the interchain spectra are sensitively affected. Above  $V_c$ , in contrast to the repulsion-strength de-

pendence, the intrachain spectra are sensitive to the interchain transfer integral, while the interchain spectra remain suppressed at low energies. These results are due to the fact that the collective motion of fermions is allowed only along the chains even if the long-range charge order is absent. Interchain coherent band motion is suppressed by electron correlation, which is analytically studied at commensurate fillings.<sup>8</sup> The interchain transfer integral weakens the charge order and facilitates the collective motion of fermions along the chains. The effect of the interchain transfer integral is somewhat similar to that of doping, when the intrachain correlation is so strong that the interchain motion of fermions is incoherent.

Similarities between the optical conductivity spectra for the TMTSF family and those calculated for a doped one-dimensional Mott insulator have been pointed out.<sup>35</sup> In the present model calculations, however, the mechanism for the insulating ground state is not spin-density-wave formation but charge ordering. Furthermore, the truly two- or three-dimensional motion of fermions observed in the TMTSF family at very low energies is beyond the scope of the present paper for coupled one-dimensional systems, and left to the future problem. Technically, the present numerical method cannot deal with the optical conductivity spectra, which are zero-momentum properties, but can treat the local spectra, in which all the momentum components are summed up.

Though the present results are obtained in the limited case of the two-leg ladder, we expect similar difference between the intrachain and interchain spectra in quasi-one-dimensional electron systems with strong intrachain electron correlation in general. It is because, both in the present study and in the TMTSF family, the umklapp process is essential to the crossover. When a gap is produced by the umklapp process *within* a chain, interchain one-particle hopping processes are strongly suppressed, as discussed in the phase diagram of quasi-one-dimensional organic conductors.<sup>8</sup> Interchain motion of electrons is thus easily frozen, and a long-range order is formed once the corresponding particle-hole processes become coherent. Meanwhile, intrachain motion of electrons is collective at low energies, inhibiting the one-body band picture. With well-developed but short-range order, the low-energy collective modes are regarded as solitons and antisolitons.

#### ACKNOWLEDGMENTS

The author is grateful to J. Kishine for fruitful discussions at the early stage of this work. This work was supported by the NEDO International Joint Research Grant Program, a Grant-in-Aid for Scientific Research (C) from Japan Society for the Promotion of Science, and a Grant-in-Aid for Scientific Research on Priority Area "Metal-Assembled Complexes" from the Ministry of Education, Culture, Sports, Science and Technology, Japan.

#### APPENDIX A: SINGLE-CHAIN CASE

In order to show the influence of the truncation procedure in the present method, here we mainly use the spinless fer-

mion model on a single chain (which is equivalent to the  $t_b = 0$  case of the model used in the text) at half filling. The single-chain model is much easier to treat and has smaller errors. The dynamical structure factor for the local charge transfer  $S_{jxjx}(\omega)$  is calculated for  $t=1.0$  and  $V=3.0$  and with different  $m$ ,  $M$ , and  $T$  values. At  $T=0.25$ , which is used in the text also, the data with  $m=14$  and with  $m=18$  are indistinguishable from each other at  $M=24$ , and those with  $M=24$  and with  $M=36$  are also indistinguishable at  $m=14$ . Thus, they converge well already at  $m=14$  and  $M=24$ . At a lower temperature,  $T=0.167$ , the low-energy spectra are slightly shifted downward due to smaller thermal fluctuations, and the difference from those at  $T=0.25$  is well developed and much larger than the numerical error.

As the interaction becomes weak, the accuracy of the present method generally becomes worse because the eigenvector of the quantum transfer matrix is numerically represented basically on site bases, more precisely speaking, on block bases since the unit block is diagonalized with respect to the block Hamiltonian. In order to check the accuracy of the spectra, we calculate them in the worst case of  $V=0$ , where the exact spectra are analytically obtained. Note that the Bethe ansatz for the single-chain spinless-fermion model and the equivalent spin-1/2  $XXZ$  model tells the ground-state properties including the quantum critical point, but it does not tell the excitation spectra for general value of  $V$ . In any case, the worst case can be exactly calculated, so that it would be enough to confirm the accuracy of the present method.

The single-particle density of states  $\rho(\omega)$  in the noninteracting case has the inverse-square-root singularity at  $\omega = \pm 2t$ , but it is rounded in the numerical spectrum. The nonsingular part is very well reproduced. The sum rule is also well satisfied. As the interaction strength increases, quantum fluctuations round the singular part, so that the present method would give more accurate results. Figure 13 shows  $\rho(\omega)$  for different  $V$ . With increasing  $V$ , the singularity is indeed more rounded, and  $\rho(\omega)$  at  $\omega=0$  decreases. The

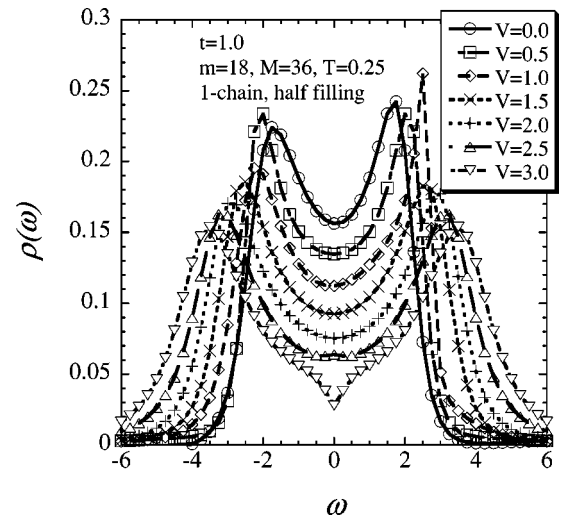


FIG. 13. Density of states in the single-chain model, for different  $V$  at half filling. The other parameters are  $t=1.0$ ,  $T=0.25$ ,  $m=18$ , and  $M=36$ .

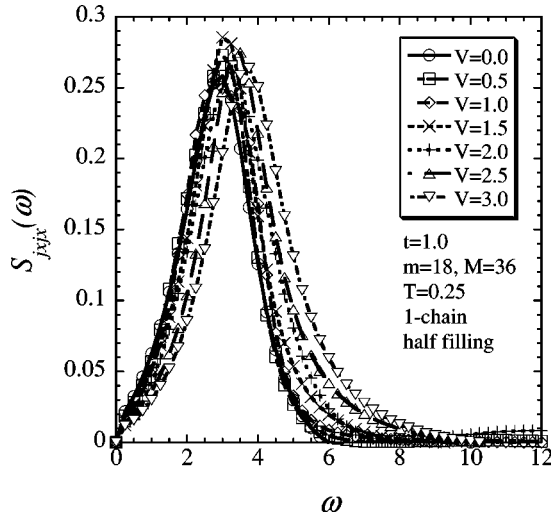


FIG. 14. Dynamical structure factor for the local charge transfer in the single-chain model, for different  $V$  at half filling. The other parameters are  $t = 1.0$ ,  $T = 0.25$ ,  $m = 18$ , and  $M = 36$ .

ground state at half filling is known to have a finite gap for  $V > 2t$ . For  $V = 2.5$ , the magnitude of the gap is estimated to be much smaller than 0.1 from the extrapolation of the ground-state DMRG results. The present calculation is performed at a finite temperature of  $T = 0.25$ , which is much larger than the gap. That is why the gap structure is completely smeared out by thermal fluctuations. For  $V = 3.0$ , there exists a gap of magnitude about 0.1, while  $\rho(\omega)$  clearly shows a pseudogap structure at a wider energy range. The gap is still smaller than the temperature, so that  $\rho(0)$  is still finite. With increasing  $V$ , the peaks in  $\rho(\omega)$  are shifted further, and located around  $\omega = \pm V$  for large  $V$ .

The dynamical structure factor for the local charge transfer  $S_{jxjx}(\omega)$  in the noninteracting case has a discontinuity at  $\omega = 4t$ , but it is rounded in the numerical spectrum. Away from this point, especially at low energies, the spectrum is well reproduced. The sum rule is well satisfied again. Figure 14 shows  $S_{jxjx}(\omega)$  for different  $V$ . The spectra  $S_{jxjx}(\omega)$  are insensitive to  $V$  for  $V < 2t$ . Especially, the low-energy side of the peak is almost independent of  $V$ , and the high-energy side is steadily and slowly shifted to further higher energies with increasing  $V$ . For  $V > 2t$ , however, the low-energy part is steadily suppressed and shows a pseudogap structure in a wider energy range than the gap. These features of  $\rho(\omega)$  and of  $S_{jxjx}(\omega)$  are observed also in the two-chain case for small  $t_b$ . Thus the one- and two-chain results are consistent with each other.

Finally, we come back to the two-leg ladder model with

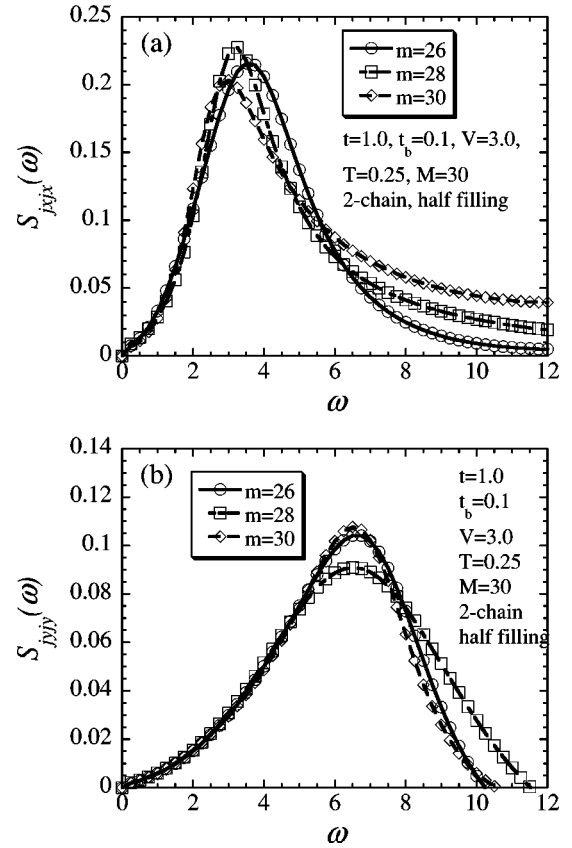


FIG. 15. Dynamical structure factor for the local charge transfer (a) along the chains and (b) across the chains, for different  $m$  at half filling. The other parameters are  $t = 1.0$ ,  $t_b = 0.1$ ,  $V = 3.0$ ,  $T = 0.25$ , and  $M = 30$ .

finite  $t_b$ . Because the degrees of freedom per unit are much more than those in the single-chain model, the numerical accuracy becomes much worse if we use the same values for  $m$  and  $M$ . Although the accuracy is still worse than that shown here in the single-chain model, we find that the values  $m = 26, 28$ , or  $30$  and  $M = 30$  semiquantitatively reproduce the overall spectral shapes rather well in the two-leg ladder model. Because the value of  $m$  is more crucial to the accuracy, we show the dynamical structure factors with different  $m$  in Fig. 15(a) for the intrachain process, and in Fig. 15(b) for the interchain process. The overall structures are not so much affected by  $m$ . Especially the spectral weight at low energies and the position of the peak converge well. However, the spectral weight and shape at high energies are generally less accurate.

<sup>1</sup>D. Jérôme, *Science* **252**, 1509 (1991).

<sup>2</sup>T. Ishiguro, K. Yamaji, and G. Saito, *Organic Superconductors* (Springer-Verlag, Berlin, 1998).

<sup>3</sup>J. Moser, M. Gabay, P. Auban-Senzier, D. Jérôme, K. Bechgaard, and J. M. Fabre, *Eur. Phys. J. B* **1**, 39 (1998).

<sup>4</sup>S. A. Brazovskii and V. M. Yakovenko, *Sov. Phys. JETP* **62**, 1340 (1985).

<sup>5</sup>C. Bourbonnais and L. G. Caron, *Int. J. Mod. Phys. B* **5**, 1033 (1991).

<sup>6</sup>D. Boies, C. Bourbonnais, and A.-M. S. Tremblay, *Phys. Rev. Lett.* **74**, 968 (1995).

<sup>7</sup>C. Castellani, C. Di Castro, and W. Metzner, *Phys. Rev. Lett.* **69**, 1703 (1992).

<sup>8</sup>J. Kishine and K. Yonemitsu, *J. Phys. Soc. Jpn.* **67**, 2590 (1998);

- 68**, 2790 (1999).
- <sup>9</sup>J. Kishine and K. Yonemitsu, *J. Phys. Soc. Jpn.* **66**, 3725 (1997); **67**, 1714 (1998).
- <sup>10</sup>V. Vescoli, L. Degiorgi, W. Henderson, G. Grüner, K. P. Starkey, and L. K. Montgomery, *Science* **281**, 1181 (1998).
- <sup>11</sup>K. Magishi, S. Matsumoto, Y. Kitaoka, K. Ishida, K. Asayama, M. Uehara, T. Nagata, and J. Akimitsu, *Phys. Rev. B* **57**, 11 533 (1998).
- <sup>12</sup>T. Takahashi, Y. Maniwa, H. Kawamura, and G. Saito, *J. Phys. Soc. Jpn.* **55**, 1364 (1986).
- <sup>13</sup>J. M. Delrieu, M. Roger, Z. Toffano, and A. Moradpour, *J. Phys. (Paris)* **47**, 839 (1986).
- <sup>14</sup>M. Uehara, T. Nagata, J. Akimitsu, H. Takahashi, N. Môri, and K. Kinoshita, *J. Phys. Soc. Jpn.* **65**, 2764 (1996).
- <sup>15</sup>J. Kishine, *Phys. Rev. B* **62**, 2377 (2000); J. Kishine and K. Yonemitsu, *ibid.* **62**, 13 323 (2000).
- <sup>16</sup>K. Yonemitsu and J. Kishine, *J. Phys. Chem. Solids* **62**, 99 (2001).
- <sup>17</sup>M. Tsuchiizu, P. Donohue, Y. Suzumura, and T. Giamarchi, *Eur. Phys. J. B* **19**, 185 (2001), and references therein.
- <sup>18</sup>S. Biermann, A. Georges, A. Lichtenstein, and T. Giamarchi, *Phys. Rev. Lett.* **87**, 276405 (2001), and references therein.
- <sup>19</sup>J. Kishine and K. Yonemitsu, *Int. J. Mod. Phys. B* **16**, 711 (2002).
- <sup>20</sup>W. Henderson, V. Vescoli, P. Tran, L. Degiorgi, and G. Grüner, *Eur. Phys. J. B* **11**, 365 (1999).
- <sup>21</sup>J. Sólyom, *Adv. Phys.* **28**, 201 (1979).
- <sup>22</sup>S. Sachdev, *Quantum Phase Transitions* (Cambridge University Press, Cambridge, 1999).
- <sup>23</sup>R. J. Bursill, T. Xiang, and G. A. Gehring, *J. Phys.: Condens. Matter* **8**, L583 (1996).
- <sup>24</sup>X. Wang and T. Xiang, *Phys. Rev. B* **56**, 5061 (1997).
- <sup>25</sup>N. Shibata, *J. Phys. Soc. Jpn.* **66**, 2221 (1997); T. Mutou, N. Shibata, and K. Ueda, *Phys. Rev. Lett.* **81**, 4939 (1998); N. Shibata and K. Ueda, *J. Phys.: Condens. Matter* **11**, R1 (1999).
- <sup>26</sup>S. R. White, *Phys. Rev. Lett.* **69**, 2863 (1992); *Phys. Rev. B* **48**, 10 345 (1993).
- <sup>27</sup>K. Yonemitsu, *Mol. Cryst. Liq. Cryst.* **376**, 53 (2002).
- <sup>28</sup>K. Yonemitsu and J. Kishine, *J. Phys. Soc. Jpn.* **69**, 2107 (2000).
- <sup>29</sup>P. Donohue, M. Tsuchiizu, T. Giamarchi, and Y. Suzumura, *Phys. Rev. B* **63**, 045121 (2001).
- <sup>30</sup>K. Yonemitsu, *Synth. Met.* (to be published).
- <sup>31</sup>For  $V=2.0$ , the peak height is substantially lower than those for  $V=1.0$  and  $V=3.0$ , but this would be due to the truncation error: we do not systematically find similar behavior for different  $m$ .
- <sup>32</sup>C. Bourbonnais, *Synth. Met.* **84**, 19 (1997).
- <sup>33</sup>Y. Suzumura, M. Tsuchiizu, and G. Grüner, *Phys. Rev. B* **57**, 15 040 (1998); M. Tsuchiizu, Y. Suzumura, and T. Giamarchi, *Prog. Theor. Phys.* **101**, 763 (1999); M. Tsuchiizu and Y. Suzumura, *Phys. Rev. B* **59**, 12 326 (1999).
- <sup>34</sup>K. Yonemitsu, *J. Low Temp. Phys.* **117**, 1765 (1999); *Mol. Cryst. Liq. Cryst.* **341**, 543 (2000); *Physica B* **284-288**, 515 (2000).
- <sup>35</sup>A. Schwartz, M. Dressel, G. Grüner, V. Vescoli, L. Degiorgi, and T. Giamarchi, *Phys. Rev. B* **58**, 1261 (1998).
- <sup>36</sup>T. Giamarchi, *Phys. Rev. B* **44**, 2905 (1991); *Physica B* **230-232**, 975 (1997).
- <sup>37</sup>M. Mori, H. Fukuyama, and M. Imada, *J. Phys. Soc. Jpn.* **63**, 1639 (1994); M. Mori and H. Fukuyama, *ibid.* **65**, 3604 (1996).